ELSEVIER

S0032-3861(96)00516-2

Polymer Vol. 38 No. 2, pp. 463–468, 1997

0032-3861/97/$17.00 + 0.00

Fine structure and tensile properties of ramie fibres in the crystalline form of cellulose I, II, III_I and IV_I

Atsuko Ishikawa* and Takeshi Okano
Department of Forest Products, Faculty of Agriculture, The University of Tokyo, Yayoi, Bunkyo-ku, Tokyo 113, Japan

and Junji Sugiyama
Division of Wood Bioscience, Wood Research Institute, Kyoto University, Uji, Kyoto 611, Japan
(Received 13 February 1996; revised 29 March 1996)

This study focuses on the change in the fine structure and tensile properties of ramie fibres by the treatment for crystalline conversion. Through the conversion from cellulose I into II, III_I and IV_I, the integral crystallinity index and the crystallite size decreased and the internal surface area increased while Young's modulus of the fibre decreased and the ultimate strain increased. Two phase parallel, series and parallel–series models which comprise two kinds of springs with different constants representing the crystalline and amorphous components, respectively, were applied to the tensile force–strain relationship of the fibres. The parallel model could not be applied to the samples because the crystal lattice strains were smaller than the fibre strains; the former strains were less than one fourth of the latter ones, at any given tensile load. On the basis of the series model, Young's modulus of crystalline component of cellulose III_I was the highest and the next was that of cellulose I, followed by II and IV_I. Young's modulus of amorphous component of cellulose I was the highest and the next was that of II, followed by III_I and IV_I. Applying a parallel–series model, the values for Young's moduli of crystalline and amorphous components were found to depend both on the feature of crystalline component and the density of amorphous region. Copyright © 1996 Elsevier Science Ltd.

(Keywords: ramie fibres; cellulose polymorphs; tensile properties)

INTRODUCTION

It is well known that cellulose can exist as the crystalline microfibrils of cellulose I, II, III and IV[1]. Cellulose I is a native form of cellulose and it is composed of I_α and I_β[2,3]. Cellulose II is easily obtained by the mercerization of native cellulose. Cellulose III and IV are derived from cellulose I and II, and they are called cellulose III_I and IV_I, III_{II} and IV_{II}, respectively. Consequently, there are at least seven crystalline forms of cellulose. It is also well accepted that those celluloses can be divided into two groups of cellulose I and II by the fact that celluloses can convert to one another in the group. Cellulose I group consists of cellulose I, III_I and IV_I, and cellulose II group consists of cellulose II, III_{II} and IV_{II}. Celluloses of the cellulose I group are able to convert irreversibly into those of the cellulose II group[4]. This irreversibility might come from the change of chain arrangement in the crystal. Namely, parallel chain arrangement of the cellulose I group changes into more stable anti-parallel one of the cellulose II group. If this is true, it may probably be said that mechanical properties of cellulose II group is superior to those of cellulose I group. Young's modulus of cellulose II crystal, however, was reported to be smaller than that of cellulose I crystal[5–8]. Those values of cellulose III and IV, scarcely reported, are smaller than that of cellulose I without exceptions[8]. Those values were conducted on the assumption that cellulose microfibrils are composed of a series of crystalline and amorphous regions. Is this assumption correct? We investigated tensile properties of ramie fibres and discussed the elastic modulus of those fibres using three mechanical models composed of two springs representing crystal and amorphous region, respectively, to make clear what caused differences in the elastic modulus among polymorphs of celluloses. We also examined the dimension of microfibrils and the inner surfaces of different celluloses to discuss relationship with the properties.

EXPERIMENTAL

Sample preparation

Purified ramie fibres supplied by Teikoku Bouseki K. K. were used as cellulose I. Cellulose II was obtained by immersing the fibres in 3.5 N NaOH solution for 2 h, followed by washing with 0°C water at ambient conditions[9]. Cellulose III_I (hereafter expressed as III for simplicity) was obtained by soaking the fibres in 75%

* To whom correspondence should be addressed

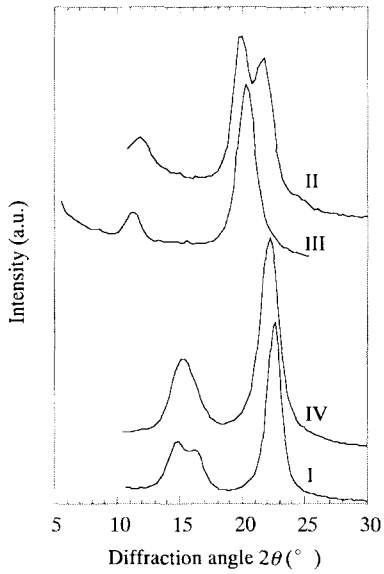

Figure 1 Equatorial diffraction curves of ramie cellulose I, II, III and IV

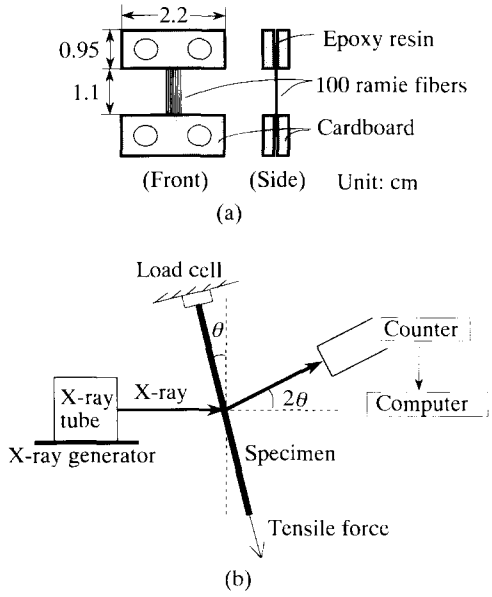

Figure 2 (a) Specimen for tensile test with X-ray diffraction. (b) Schematic representation of X-ray diffractometry

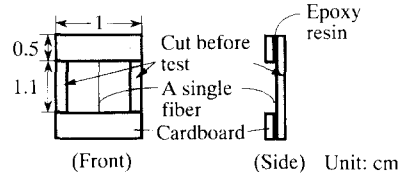

Figure 3 Specimen for tensile test of a single fibre

ethylenediamine for 1 h, followed by rinsing with 99% methanol[10]. Each procedure was repeated until the respective fibre yielded the typical X-ray diagrams. Cellulose IV_I (hereafter expressed as IV for simplicity) was prepared by immersing cellulose III in glycerol for 3 days, followed by heating at 260°C in an autoclave for 30 min and washing with water and acetone successively[11]. *Figure 1* shows the X-ray equatorial diffraction curves for each sample. The density of these samples measured with a pycnometer in xylene–carbon tetrachloride as a medium was 1.58 for cellulose I, 1.55 for II, 1.49 for III and 1.51 g cm^{-3} for IV. A bundle of one hundred ramie fibres as illustrated in *Figure 2a* was used for X-ray measurements.

X-ray diffractometry and determination of diffraction profiles

X-ray measurements were made with a symmetrical transmission technique previously reported[12]. Ni filtered Cu K_α radiation ($\lambda = 0.1542$ nm) generated at 40 kV and 80 mA by a Rigaku RU-200BH generator was collimated through a pinhole collimator of 2 mm ϕ with a length of 7.5 cm. The diffracted beam was detected by a scintillation counter with a pulse-height analyzer at 0.5° min^{-1}. The diffraction intensity and the force applied to the specimen were recorded on a digital recorder at the interval of one point s^{-1}.

The reflection profile of 004 was derived by subtracting background scattering assumed to be parabolic from the meridional diffraction curve and fitting with a Gaussian by the least squares. The equatorial intensity curve was likewise decomposed into three characteristic reflections of $1\bar{1}0$, 110 and 200, with background scattering assumed to be composed of two Gaussian profiles.

Integral crystallinity index and crystallite size

The integral crystallinity index was evaluated as the ratio of the sum of integrated intensities of $1\bar{1}0$, 110 and 200 reflections to total integrated intensity in the range of $2\theta = 10$–$30°$ for cellulose I, II and IV and $2\theta = 5$–$25°$ for cellulose III, respectively. The crystallite size was calculated from $1\bar{1}0$ and 110 reflection profiles based on Scherrer's equation[13] corrected by NaF reflection.

Crystal lattice strain (ϵ_c)

Crystal lattice strain in the longitudinal direction was derived from deformation of 004 d-spacing induced by the force applied to the specimen. The deformation of d-spacing was calculated from the shift of the diffraction angle 2θ relative to the (004) plane by the following equation obtained by differentiating Bragg's equation.

$$\epsilon_c = \frac{\Delta d}{d} = -\Delta\theta \cot \theta \qquad (1)$$

where d is d-spacing.

Young's modulus, ultimate strength and strain of the fibres

A single fibre 11 mm long was clamped between pieces of cardboard with epoxy resin as shown in *Figure 3*. Tensile testing was performed on a universal testing machine (Tensilon UTM-III-100, Toyo Baldwin Co., Ltd., Tokyo, Japan) at 65% RH, 20°C. The specimen was fastened with air chucks, and then both lateral sides of the cardboard frame were cut just before testing. Tensile speed was 10 mm min^{-1}. In order to evaluate stress applied to the specimen the cross-sectional area of a fibre was carefully measured as follows. The fibre was put on double sided tape pasted on a transparency sheet and covered with another transparency sheet. Then the fibre was cut along its cross section and coated with gold for SEM (JEOL Ltd., Tokyo, Japan, S-4000) observation. The cross-sectional areas of the samples were recorded on photograph, then scanned into a computer and calculated by means of image analysing software.

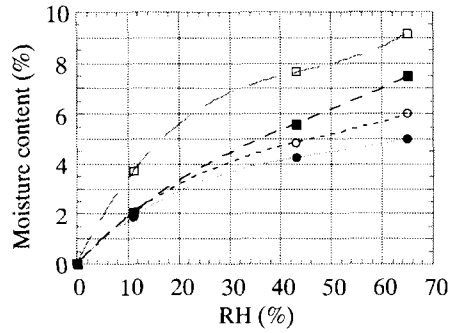

Figure 4 Hygroscopic isotherms of cellulose I, II, III and IV. –●– : Cellulose I, —⊟- - : cellulose II, — ■- - : cellulose III, - - ⊖ - - : cellulose IV

Table 1 Properties of ramie cellulose I, II, III and IV

	Crystallinity index (%)	Crystallite width (nm)	Crystallite length (nm)	Internal surface area ($m^2 g^{-1}$)
Cellulose I	64 (100)[a]	4.8 (100)	18.7 (100)	133 (100)
Cellulose II	53 (83)	5.1 (106)	15.4 (82)	229 (172)
Cellulose III	38 (59)	5.1 (106)	15.0 (80)	184 (138)
Cellulose IV	57 (89)	3.8 (79)	16.1 (86)	153 (115)

[a] Ratio to the value for cellulose I

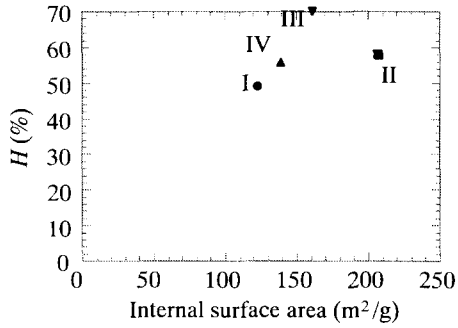

Figure 5 Relationship between calculated percentage of amorphous region (*H*) and internal surface area of ramie cellulose I, II, III and IV

Table 2 Tensile properties of ramie fibres

	E_f^a (GPa)	σ_b^b (MPa)	ε_b^c ($\times 10^{-2}$)
Cellulose I	27	755	3.2
Cellulose II	21	798	5.0
Cellulose III	15	693	5.8
Cellulose IV	13	345	5.0

[a] E_f: Young's modulus of a single fibre
[b] σ_b : Strength
[c] ε_b: Ultimate strain

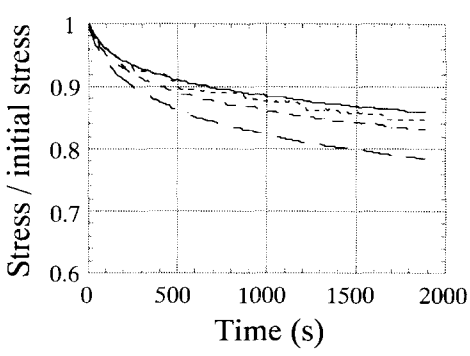

Figure 6 Stress relaxation curves for ramie cellulose I, II, III and IV. ——: Cellulose I, — — —: cellulose II, – – –: cellulose III, - - - -: cellulose IV

Young's modulus, ultimate strength and ultimate strain were evaluated. Up to a total number of 50, the measurements were carried out with the samples.

Measurements of internal surface area of the fibres

Hygroscopic isotherms of the fibres were obtained (*Figure 4*): equilibrium moisture contents of the specimens in desiccators with P_2O_5, saturated solutions of LiCl and K_2CO_3 (0, 11, 43 RH, respectively) were recorded to the relative humidity. Then the internal surface area of the fibres in the respective crystalline forms was evaluated according to BET theory[14].

RESULTS AND DISCUSSION

Fine structure of the fibres and crystallite sizes

Integral crystallinity index (*CrI*) and internal surface area of the fibres, and crystallite size are listed in *Table 1*. The integral crystallinity index decreased and the internal surface area increased by the treatment of crystal conversion from cellulose I to the other forms, while the crystallite width almost remained unchanged except cellulose IV. This result indicates that decrystallization occurred in the longitudinal direction by the conversion treatment. Remarkable increase of integral crystallinity index was observed in the formation of cellulose IV. This is compensated not by decomposition but by crystallization of amorphous component through the heat treating of cellulose IV. The internal surface area of cellulose II seems to be rather high. We estimated, therefore, the ratio (*H*) of amorphous chains to the total chains using integral crystallinity index and crystallite size. A half number of the crystal chains which exist on the surface of the crystallite was assumed to be amorphous ones. Consequently, the ratio was estimated by the following equation.

$$H = \frac{\frac{1}{2} W_{sc}}{W_c} CrI + (1 - CrI) \qquad (2)$$

where W_{sc} is number of the cellulose chains which exist on the crystallite surface, W_c is total number of cellulose chains in the crystallite. The ratios *H* of cellulose I, III and IV seem to be proportional to the internal surface area, whereas *H* of II deviates from the others (*Figure 5*). The fact indicates that crystallite of cellulose II is more imperfect. Otherwise, amorphous component of ramie cellulose II would be more hydrophilic.

Tensile properties of fibres

Basic data on tensile properties of the fibres are shown in *Table 2*. Young's modulus of the fibre (E_f) decreased 20–50% and the ultimate strain (ϵ_b) increased more than 50% through the conversion from cellulose I to the other forms. We will discuss this data in detail later.

Two-phase model interpretation

Ramie fibres showed stress relaxation behaviour when the fibres were constrained a constant length as in *Figure 6*. These stress relaxation behaviours can be generally represented by mechanical models with dashpots. Since the crystallite strain was measured after the stress relaxation had almost ended, we could adopt the models comprising springs without dashpots, which might be able to make the discussion easier.

Firstly, a parallel model was examined. Crystalline

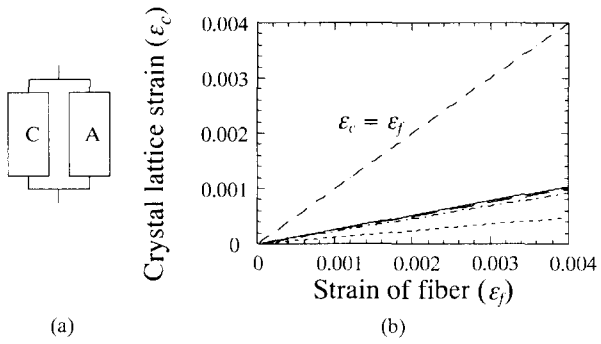

Figure 7 (a) Parallel model. (b) Relationship between crystal lattice strain and strain of a single fibre. ———: Cellulose I, — — —: cellulose II, - - - - -: cellulose III, – – – –: cellulose IV

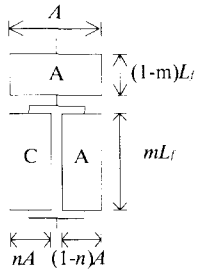

Figure 8 Parallel–series model

and amorphous components in the model of fibres are represented by rods, C and A. This parallel model shown in *Figure 7* requires the crystal lattice strain (ϵ_c) and the fibre strain (ϵ_f) to be equal when the fibres were strained. However, the value for ϵ_c was smaller than one fourth of ϵ_f shown in *Figure 7*. This result strongly suggests that the parallel model is not applicable to the fibres.

Next, we examined a series–parallel model shown in *Figure 8*. This model consists of one crystal and two amorphous rods. Elongation Δ_f of the fibre rod by tensile load P is expressed with length L_f, cross-sectional area A, compliance E_f.

$$\Delta_f = \frac{PL_f}{AE_f} \tag{3}$$

This is equal to the sum of elongation of the crystal and the amorphous rods,

$$\Delta_f = \Delta_c + \Delta_a \tag{4}$$

Those are expressed in a same fashion with the fibre,

$$\Delta_c = \frac{P_c mL_f}{nAE_c} \tag{5}$$

$$= \frac{(P - P_c)mL_f}{(1-n)AE_a} \tag{6}$$

$$\Delta_a = \frac{P(1-m)L_f}{AE_a} = \Delta_f - \Delta_c \tag{7}$$

where P_c is tensile load applied to the crystal rod, m and n are ratios of length and cross-sectional area of the crystal rod to those of the fibre rod, respectively, and E_c and E_a are Young's modulus of the crystal and amorphous rod, respectively. We can measure strain, ϵ_c, of the crystal rod, therefore as

$$\Delta_c = mL_f\epsilon_c \tag{8}$$

By substituting $\Delta_f = L_f\epsilon_f$ into the above equations, and eliminating P, P_c and A, we can represent Young's modulus E_c, E_a with E_f of the fibre rod as

$$\frac{E_c}{E_f} = \frac{1}{n}\left\{\frac{1}{k} - \frac{(1-m)(1-n)}{1-km}\right\} \tag{9}$$

$$\frac{E_a}{E_f} = \frac{1-m}{1-km} \tag{10}$$

where $k = \epsilon_c/\epsilon_f$. We can derive an equation among densities, ρ_f, ρ_c and ρ_a of the fibre, the crystal and the amorphous rods,

$$\rho_f = mn\rho_c + (1-mn)\rho_a \tag{11}$$

further, using integral crystallinity index CrI

$$\rho_f CrI = mn\rho_c \tag{12}$$

Density of the amorphous rod is derived from equations (11) and (12),

$$\rho_a = \frac{\rho_c\rho_f(1-CrI)}{\rho_c - \rho_f CrI} \tag{13}$$

The values of ρ_a were 1.49, 1.47, 1.45 and 1.40 g cm^{-3} for ramie cellulose I, II, III and IV, respectively. The value ρ_c was calculated from unit cell parameter[15–17]. Using equations (9), (10) and (12), E_c and E_a vs. n for each sample were shown in *Figures 9* and *10*. The series model $n = 1$ in the parallel–series model, gives the values for E_c

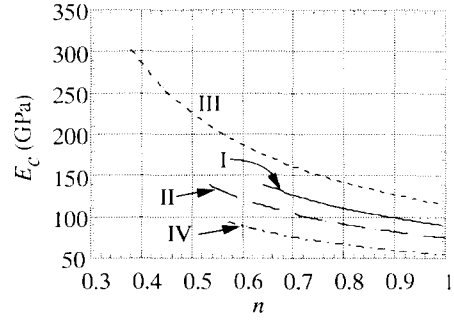

Figure 9 Relationships between Young's modulus of crystalline component (E_c) and ratio of cross-sectional area of the crystalline component to that of the fibre (n) in the parallel–series model shown in *Figure 8*. ———: Cellulose I, — — —: cellulose II, - - - - -: cellulose III, – – – –: cellulose IV

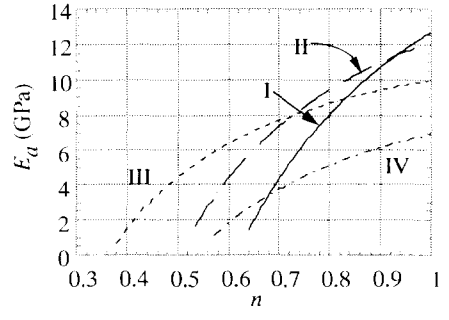

Figure 10 Relationships between Young's modulus of amorphous component (E_a) and ratio of cross-sectional area of the crystalline component to that of the fibre (n) in the parallel–series model shown in *Figure 8*. ———: Cellulose I, — — —: cellulose II, - - - - -: cellulose III, – – – –: cellulose IV

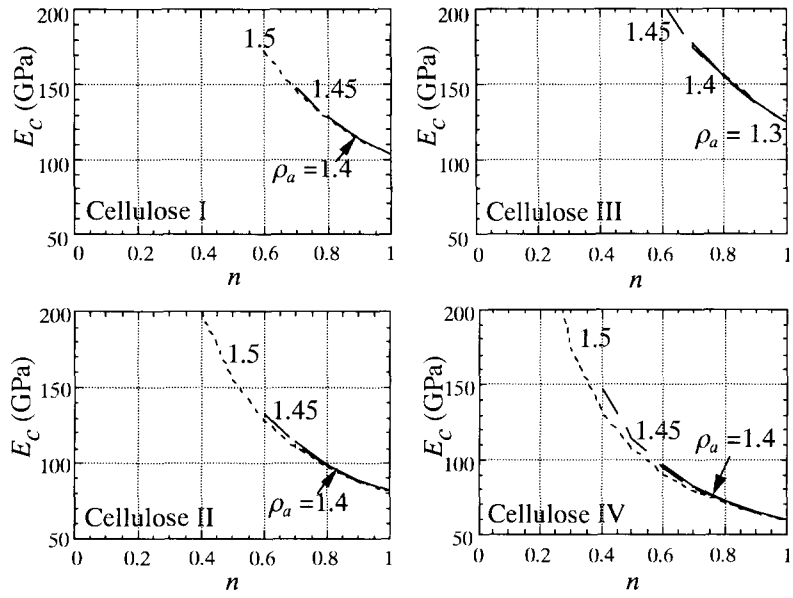

Figure 11 Young's modulus of crystalline component (E_c) as a function of ratio of cross-sectional area of the crystalline component to that of the fibre (n) with parameter of density of amorphous component (ρ_a) based on the parallel–series model shown in *Figure 8*

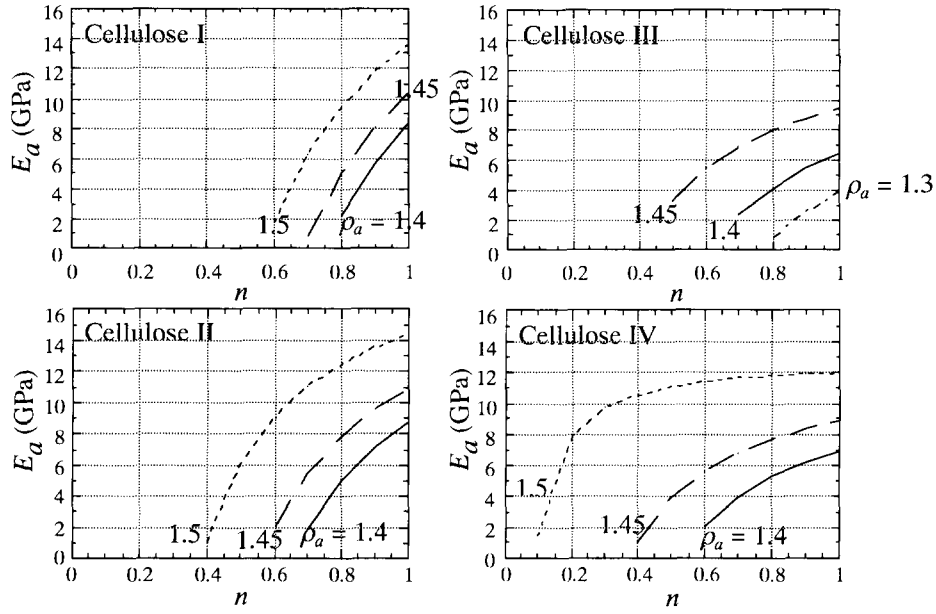

Figure 12 Young's modulus of amorphous component (E_a) as a function of ratio of cross-sectional area of the crystalline component to that of the fibre (n) with parameter of density of amorphous component (ρ_a) based on the parallel–series model shown in *Figure 8*

of cellulose I, II, III and IV (hereafter expressed as E_cI, E_cII, E_cIII and E_cIV) as 90, 75, 115 and 54 GPa, and the values for E_a of cellulose I, II, III and IV (hereafter expressed as E_aI, E_aII, E_aIII and E_aIV) as 13, 12, 10 and 7 GPa respectively. Except III, the values for E_c are rather small comparing with previously reported[5–8]. Namely, 120–138 for E_cI, 88–112 for E_cII and 75 for E_cIV. We can see the value of 87 GPa for E_cIII reported by Nishino *et al.*[8]. We demonstrated that the values for E_c and E_a will change by the structural feature of crystallite. Possible values are 90–140, 75–139, 115–302 and 54–94 GPa for E_cI, E_cII, E_cIII and E_cIV, respectively, and 1–13, 2–12, 1–10 and1–7 GPa for E_aI, E_aII, E_aIII and E_aIV.

Next, we calculated values for E_c and E_a as a function of n and ρ_a on the basis of the parallel–series model without using *CrI*. *Figures 11* and *12* show that Young's moduli of crystalline and amorphous components decrease and increase, respectively, with increasing of n, and these values can be higher range with larger value of ρ_a. Here ρ_a can be given any value but we adopted a probable value of 1.3–1.5 g cm^{-3} as example. The series model, $n = 1$ in the model, gives 114, 89, 138 and 65 GPa as E_cI, E_cII, E_cIII and E_cIV, respectively. Consequently, Young's modulus of cellulose crystallite will be decided when we can estimate both the crystal feature and the density of the amorphous component.

Finally, we considered the relationship between the irreversibility of the crystalline conversion from cellulose I group to II and Young's modulus of cellulose I group

and II. Young's modulus of cellulose II is not always higher than that of cellulose I group, depending on the width and density of amorphous component in the parallel–series model. It was suggested that the changes in the lengths of intramolecular hydrogen bonds induced by the crystal transition will cause changes in the crystal moduli of cellulose polymorphs[8]. Consequently, the packing energy of crystal, which concerns irreversibility of crystalline conversion from cellulose I group to II group, is not directly related to Young's modulus of crystal.

CONCLUSIONS

The integral crystallinity index and the crystallite size decreased and the internal surface area increased while Young's modulus of the fibres decreased and the ultimate strain increased, through the conversion from cellulose I into II, III and IV. Imperfection of cellulose II crystallite or high ability of adsorption of amorphous region in ramie cellulose II was indicated by the comparison of crystallite size and internal surface area. According to the calculation using integral crystallinity index, density of amorphous region of ramie cellulose I is the highest, the next was that of II followed by III and IV. Parallel model comprising crystalline and amorphous component could not be applied to the samples. On the basis of the series model, E_cIII is the highest and the next is E_cI followed by E_cII and E_cIV, and E_aI is the highest and the next is E_aII followed by E_aIII and E_aIV. Using parallel–series model, we demonstrated that the values for E_c and E_a will change by these structural features of crystallite. Young's modulus of cellulose II is not always higher than that of cellulose I group. Consequently, Young's modulus of crystal does not directly reflect the lower packing energy of cellulose II than that of cellulose I group.

REFERENCES

1 Sarko, A. *Tappi* 1978, **61,** 59
2 Atalla, R. H. and VanderHart, D. L. *Science* 1984, **223,** 283
3 VanderHart, D. L. and Atalla, R. H. *Macromolecules* 1984, **17,** 1465
4 Hayashi, J. in 'CELLULOSE. Structural and Functional Aspects' (Eds J. F. Kennedy, G. O. Phillips and P. A. Williams), Ellis Horwood Limited, John Wiley & Sons, 1989, p. 35
5 Sakurada, I. and Ito, T. *Koubunshikagaku* 1962, **19,** 300
6 Sakurada, I. and Kaji, K. *J. Polym. Sci., Part C* 1970, **31,** 57
7 Matsuo, M., Sawatari, C., Iwai, Y. and Ozaki, F. *Macromolecules* 1990, **23,** 3266
8 Nishino, T., Takano, K. and Nakamae, K. *J. Polym. Sci., Part B: Polym. Phys.* 1995, **33,** 1647
9 Kim, N.-H., Sugiyama, J. and Okano, T. *Mokuzai Gakkaishi* 1991 **37,** 637
10 Lokhande, H. T., Shukla, S. R., Chidambareswaran, P. K. and Patil, N. B. *J. Polym. Sci., Polym. Lett. Ed.* 1977, **15,** 97
11 Isogai, A., Usuda, M., Kato, T., Uruy, T. and Atalla, R. H. *Macromolecules* 1989, **22,** 3168
12 Moriizumi, S. and Okano, T. *Mokuzai Gakkaishi* 1978, **24,** 1
13 Alexander, L. E. in 'X-ray Diffraction Methods in Polymer Science', John Wiley & Sons, 1969, p. 423
14 Brunauer, S., Emmett, P. H. and Teller, E. *J. Am. Chem. Soc.* 1938, **60,** 309
15 Woodcock, C. and Sarko, A. *Macromolecules* 1980, **13,** 1183
16 Wellard, H. J. *J. Polym. Sci.* 1954, **13,** 471
17 Sarko, A., Southwick, J. and Hayashi, J. *Macromolecules* 1976, **9,** 857

NOMENCLATURE

ϵ_c	crystal lattice strain
d	d-spacing
CrI	integral crystallinity index
H	ratio of amorphous chains to the total chains in the fibre
W_{sc}	number of the cellulose chains which exist on the crystallite surface
W_c	total number of cellulose chains in the crystallite
E_f	Young's modulus of the fibre
ϵ_b	ultimate strain
Δ_f	elongation of the fibre
P	tensile load
L_f	length of series–parallel model
A	cross-sectional area of series–parallel model
Δ_c	elongation of the crystal rod in series–parallel model
Δ_a	elongation of the amorphous rod in series–parallel model
P_c	tensile load applied on the crystal rod in series–parallel model
m	ratio of length of the crystal rod to that of the fibre rod in series–parallel model
n	ratio of cross-sectional area of the crystal rod to that of the fibre rod in series–parallel model
E_c	Young's modulus of the crystal component
E_a	Young's modulus of the amorphous component
k	ratio of crystal lattice strain to strain of the fibre
ϵ_f	strain of the fibre
ρ_f	density of the fibre
ρ_c	density of the crystal component
ρ_a	density of the amorphous component
E_cI, E_cII, E_cIII and E_cIV	Young's modulus of cellulose I, II, III and IV crystal, respectively
E_aI, E_aII, E_aIII and E_aIV	Young's modulus of amorphous component in ramie cellulose I, II, III and IV, respectively